Research Square

Preprints are preliminary reports that have not undergone peer review.
They should not be considered conclusive, used to inform clinical practice,
or referenced by the media as validated information.

Elevation differences in aerosol impact on extreme precipitation

Birthe Marie Steensen

birthe.steensen@cicero.oslo.no

Center for International Climate Research: CICERO https://orcid.org/0000-0001-9664-1635

Kari Alterskjær

Center for International Climate Research: CICERO

Camilla Weum Stjern

Center for International Climate Research: CICERO

Trude Storelvmo

University of Oslo Faculty of Mathematics and Natural Sciences: Universitetet i Oslo Det Matematisk-naturvitenskapelige Fakultet

Erich Fischer

ETH Zurich Department of Civil Environmental and Geomatic Engineering: Eidgenossische Technische Hochschule Zurich Departement Bau Umwelt und Geomatik

Research Article

Keywords:

Posted Date: June 4th, 2026

DOI: https://doi.org/10.21203/rs.3.rs-9452377/v1

License: This work is licensed under a Creative Commons Attribution 4.0 International License.
Read Full License

Abstract

Understanding how aerosols influence extreme precipitation is critical for predicting flood risks, water availability and management in regions with complex topography. Here we present results from two parallel model simulations with convection-permitting resolution with different aerosol loadings over Germany. We find that daily extreme precipitation gives opposite response to aerosol reductions with elevation height; with cleaner air we find an increase below 150 m of elevation while there is a decrease in daily extremes above 150 m. German station data show the same pattern where trends in annual maximum precipitation reverse sign before and after the 1980s peak in anthropogenic aerosol pollution, with opposite trend directions for stations below and above 150 m. Model results show that the conditions at higher elevations are more favorable for activating cloud droplets, enhancing droplet freezing and in turn snow production. This strengthens updrafts more efficiently in polluted conditions, producing more precipitation from the start of the day, until the afternoon. Despite the contrasting daily response to aerosol loading with elevation, the effect of aerosol reductions on hourly extremes is similar across the elevations with shorter, more intense precipitation and potentially greater damage potential. These findings highlight the importance of accounting for aerosol–cloud interactions and topography when assessing regional precipitation extremes and flood risk.

1. Introduction

Europe has experienced an increase in extreme precipitation over the recent decades (Fischer and Knutti, 2016; Myhre et al., 2019; Seneviratne et al., 2021; Sun et al., 2021), with growing impacts on society. These effects can be particularly severe in mountain regions, where extreme rainfall threatens freshwater resources and increases the risk of flash floods and landslides (Archer and Fowler, 2018; Borga et al., 2005; Gaume et al., 2009). A recent example is the July 2021 flooding in western Germany and Belgium, which resulted in widespread damage and more than 200 fatalities, underscoring the severe societal impacts of extreme rainfall (Kreienkamp et al., 2021). Although the intensification of mean and extreme precipitation is primarily driven by large-scale warming, emerging evidence suggests that aerosols may modulate these changes (Andrews et al., 2010; Samset, 2022). Aerosols affect precipitation both globally and regionally (Zou et al., 2025). For example, reductions in incoming solar radiation over global land surfaces from 1960 to 1990 have been reported to cause a deacceleration of the hydrological cycle (Wild, 2009). Europe experienced rising aerosol concentrations until the mid-1980s, followed by a rapid decline in subsequent decades (Hoesly et al., 2018). The extent to which these changes have influenced extreme precipitation, particularly across mountainous and lowland regions, remains uncertain.

Changes in pollution that cause aerosols acting as Cloud Condensation Nuclei (CCN) affect the formation and evolution of droplets in clouds, and in turn how precipitation is formed. Higher concentrations of CCN lead to higher concentrations of cloud droplets competing for the same available water vapor, resulting in smaller droplets. These smaller droplets also cause cloud brightening with increased reflection of solar radiation compared to large droplets (Twomey, 1977). Smaller droplets have

lower collision-coalescence efficiency, which reduces warm rain formation (Albrecht, 1989; Squires, 1958), and thus has the potential for delaying precipitation onset. In mixed-phase clouds, smaller droplets can persist as supercooled liquid, promoting freezing at higher altitudes and releasing latent heat aloft, thereby strengthening updrafts, and potentially enhancing precipitation intensity (Altaratz et al., 2014). Once ice forms, growth of ice crystals at the expense of supercooled droplets through the Bergeron-Findeisen process and riming can further accelerate precipitation. The strong dependence of these processes on ambient thermodynamic and microphysical conditions suggests that aerosol effects on extreme precipitation may vary markedly between lowland and higher-elevation regions.

Orographic effects on cloud formation and precipitation, and their interaction with aerosols adds further uncertainty. Typically, orographic lifting enhances condensation and cloud formation (Roe, 2005). This influence depends on timescale: while orography generally enhances continuous precipitation, it tends to suppress shorter duration (< = hour) precipitation associated with convective peaks (Formetta et al., 2022). Positive precipitation trends due to global warming in the mountains are found to be weaker than for low elevations by using gridded observational datasets and ERA5 reanalysis (Pepin et al., 2022). How orographic effects are impacted by aerosols is unclear. Previous studies indicate that increased aerosol loading may delay precipitation onset and reduce total precipitation in mountainous regions worldwide (Choudhury et al., 2019; Rosenfeld et al., 2007), including during extreme summer events in the Alps (Eirund et al., 2022). Results have also shown that the presence of ice phase has a large impact on the sign of the aerosol effect (Zubler et al., 2011). Napoli et al., (2019) found an orographic enhancement of observed mean precipitation in the Alps from 1950 up to the 1980s with a decline in the following decades. The authors propose that the divergent trends in aerosol loading over Europe are the cause, thus aerosols may affect precipitation differently over the mountains and the lowlands.

Here we test this hypothesis in high resolution, convection-permitting models (< 4 km grid scale), which better represent the spatial and diurnal patterns of precipitation over the Alps compared to regional models with parameterized convection (Ban et al., 2021). This has important implications for the representation of sub-daily orographic precipitation effects (Kendon et al., 2021; Lucas-Picher et al., 2021; Prein et al., 2017). In this study we investigate the impact of aerosol reductions on extreme precipitation by running two parallel 20-year simulations with the Weather Research and Forecasting (WRF) model with a convection-permitting resolution. Simulations are conducted over Germany, with clean and polluted hygroscopic water friendly aerosols acting as CCN (Thompson and Eidhammer, 2014). We separate the analysis into lowland conditions (elevations < 150 m) and conditions in terrain with hills and mountain (> 150 m, hereafter referred to as mountain conditions) to isolate and compare the respective influences of aerosol loading and elevation.

By analyzing the aerosol impact over an extended time-period (20-years) in simulation pairs driven by the same lateral boundary conditions. The results are based on several extreme events making the results more robust, compared to analyzing one event. The microphysical difference between clean and polluted conditions is studied to identify the reasons for the different responses in mountains and in lowlands.

The next section describes the data, model and methods used in this manuscript, then results are presented with discussion and conclusion in the end.

2. Data and Methods

2.1 Model

Model simulations on convection permitting scales are performed with the WRF model version 4.3 (Skamarock and Klemp, 2008). The simulations (2001–2020) are run with ERA5 (Hersbach et al., 2020) data as initial and boundary conditions, downscaled to an outer 15 km resolution domain and an innermost convection permitting 3 km domain. The two parallel simulations only differ from each other in the prescribed aerosol loading, with one representing 1980 levels (polluted) and one representing 2020 levels (clean). Water friendly aerosol number concentrations for the respective years are derived from OsloCTM3 (Oslo Chemical Transport model) (Lund et al., 2018; Skeie et al., 2020). Non-hygroscopic, ice-nucleating natural dust aerosols are kept constant between the clean and polluted runs. Each model year is run separately with a month spin-up (December), which is disregarded. Model simulations are also described in Alterskjær et al. (in review), with model validation against observations.

In order to analyze the effect of pollution on extreme precipitation, the aerosol aware microphysics scheme described in Thompson et al. (2008) and Thompson and Eidhammer (2014) is applied. The Thompson scheme enables the possibility to explicitly incorporate aerosol tracking in a more cost-effective manner compared to the fully coupled chemistry version of WRF (Thompson and Eidhammer, 2014). The radiative effective radii of cloud water, cloud ice and snow is included by coupling the microphysical scheme and the RRTMG (Rapid Radiative Transfer Model Global) (Thompson et al., 2016), in addition to the direct effect of the aerosol provided by OsloCTM3.

The five-boundary grid-cells in the innermost domain are disregarded, and only land grid cells are studied. The domain was set up to analyze the effects of aerosol on a continental area with good observational coverage, therefore northern Germany were chosen. Most of the grid cells are at an altitude below or equal to 150 m (58%), referenced to lowlands further in the results, while 37% are above 150 m, references as mountains. The remaining grid cells are ocean, see Supplementary Fig. 1.

2.2 Observations

Rx1day (annual maximum one day precipitation) trends for German stations (1313) are studied from the European Climate Assessment and Dataset (ECA&D) (Klein Tank et al., 2002), differentiated by the same elevations (above and below 150 m). Only stations with 80% coverage from 1955–2020 are analyzed and 80% of the year needs to be included for the Rx1day to be included. Linear regression trends are calculated for Rx1day over the years for stations within the two respective elevations.

2.3 Methods

For the WRF simulations, the effect of aerosol on precipitation and extreme precipitation is analyzed by examining the relative change between the clean and polluted simulations. For mean precipitation and Rx1day, the change is found in each grid cell and then averaged over the lowlands and mountains given by the grid cell elevation. In addition, we study a set of increasingly severe precipitation extremes, defined as events exceeding selected percentile thresholds of daily precipitation. This allows us to quantify changes in the amount, frequency, and intensity of extreme events across several extremes. For the percentile analysis, thresholds are determined from the clean simulations for each grid cell; for example, the 99.7th percentile represents the 21 most extreme events, with the threshold defined by the least extreme of these events (following Myhre et al., (2019) and Steensen et al., (2025)). Precipitation amount is defined as the total precipitation accumulated above the clean-simulation threshold and frequency as the number of events exceeding the same threshold. Intensity is defined as the daily precipitation of extreme events, calculated using percentile thresholds derived separately for the clean and polluted simulations so that the same number of events is included in each case. Description of the metrics used for extreme precipitation in this study is presented in Table 1. Relative changes in these metrics are then computed by comparing the clean and polluted simulations. All quantities are calculated in each grid cell and subsequently averaged over grid cells in the lowland and mountain regions. The Wilcoxon two-sided test is used to check if the results are statistically significant.

Table 1
Metrics used for extreme precipitation for the daily precipitation percentile thresholds and sub-day analysis.

Metric	Description
Rx1day	The annual maximum of daily accumulated precipitation
Precipitation amount	Total precipitation amount accumulated above the clean-simulation threshold
Intensity	Total precipitation amount accumulated over the same number of events
Frequency	Number of events above the clean-simulation threshold
Duration	The mean hourly (hours > = 1 mm/h) precipitation duration length
Maximum	The mean hourly maximum accumulated precipitation

3. Results

Figure 1 Top row shows modelled relative change in precipitation amount (green), intensity (purple) and frequency (orange) of mean and extreme precipitation between the polluted and clean simulations from the convective permitting WRF simulations for grid cells below (a) and above 150 m elevation (b). Hatched bars show statistical significance ($p < 0.05$) using the two-sided Wilcoxon test. Bottom row shows observed five-year running mean Rx1day (grey) from 1955–2020, as well as linear trends over the full period (orange), from 1955–1984 (light green) and from 1991–2020 (pink), for stations below (c) and above 150 m elevation (d), respectively.

Figure 1a) and b) shows how mean and daily extreme precipitation respond to aerosol reductions in the lowlands and the mountains in the WRF model simulations for the convective permitting 3 km domain. Cleaner air in the lowlands leads to an increase in mean and daily extreme precipitation across all metrics. In the mountains, however, we find an opposite effect (Fig. 1b); cleaner air causes a reduction in precipitation on almost all the statistics.

Observations also support an elevation-dependent response of extreme precipitation to aerosols. This is shown by investigating trends in Rx1day for German observational sites before and after the peak in pollution in the 1980s. Figure 1c) and d) show that over the 66-year period from 1955 to 2020, Rx1day shows an overall increasing trend in both elevation ranges, a signal expected from global warming, though with higher extreme precipitation values in the mountains. However, investigating the first and last 30 years individually, representing time periods with increasing and decreasing pollution, the trends are opposite to each other. In the lowlands from 1955 to 1984, German stations show a decreasing trend with − 0.021 mm/year (Supplementary Table 1), while over the last 30 years the trend is positive with 0.023 mm/year. For the German stations above 150 meters, the trend for the first 30 years is positive (0.092 mm/year) while over the last 30 years its negative (-0.036 mm/year). In other words, observations seem to reflect what we find in the model simulations; a tendency that cleaner air is associated with more extreme daily precipitation in the lowlands, while the relationship is opposite at higher elevations. In other words, despite their high year-to-year variability, observations seem to reflect what we find in the model simulations; a tendency that cleaner air is associated with more extreme precipitation in the lowlands, while the relationship is opposite at higher elevations

The elevation-dependent responses to cleaner air found in both the model simulations and observations are investigated further using the WRF simulations, focusing primarily on the average of events above the 99.7 threshold for both the clean and polluted simulations. The 99.7th percentile corresponds approximately to the most extreme daily precipitation event per year and is therefore analogous to the commonly used Rx1day metric. This comparison is analogous to the intensity metric as the identical number of events is considered in both cases.

Orographic effects is found to be time scale dependent with more precipitation on daily time-scales while orography suppress the hourly maximum precipitation associated with convective peaks (Formetta et al., 2022). Figure 2a) shows the diurnal cycle of hourly precipitation in clean conditions for days above the 99.7 percentile threshold, for lowlands (blue) and mountains (green). Both elevations show on average a small peak in the morning with a larger peak in the afternoon. The model simulations again indicate a positive orographic effect with more extreme precipitation in the mountains, and the precipitation duration is also longer in the mountains (Fig. 2b). Supporting Formetta et al., (2022), the maximum hourly precipitation amounts are comparable across both elevation ranges (Fig. 2c), however slightly higher for the highest percentile in the lowlands.

To isolate the effect of aerosol over the two elevations, the bottom row of Fig. 2 shows differences between clean and polluted conditions. The clean simulations produce less precipitation in the

mountains (see below-zero values for the green line in Fig. 2d) from the start of the day until 15:00 in the afternoon. Later in the afternoon, there is more precipitation under clean conditions. In the lowlands there is on average more extreme precipitation in the clean simulations with delayed onset of precipitation in the morning and afternoon, shown as a negative difference in the curve in the hours after the peaks. The duration of events is shorter in the clean simulations for both elevations and across the percentiles (Fig. 2e). Since the maximum hourly precipitation is on average occurring in the afternoon when it precipitates more under clean conditions, the mean maximum precipitation is higher in the clean simulations over both elevations and across the percentiles shown here (Fig. 2f).

The effect of aerosols on hourly maxima is therefore similar over the elevations, with intensified shorter duration and higher maximum in the clean simulations. However, the decrease in aerosol affects the daily accumulated extreme precipitation differently in the mountains.

To disentangle the physical mechanisms that induce differing aerosol-precipitation responses in lowlands and mountains, we take a closer look at mountain changes in relevant microphysical parameters averaged over the events above the 99.7 percentile. Figure 3 shows the mixing ratios averaged over the mountain grid cells for the five hydrometeors in the Thompson scheme; cloud water, cloud ice, rain, snow and graupel for clean aerosol conditions and how these change when going from clean to polluted conditions. The mixing ratios for snow and cloud water are higher compared to the other species, while cloud ice has the lowest mixing ratio (Figs. 3a-d). However, when comparing the relative change between clean and polluted conditions for the species, the differences are comparable around 10–20% over the daily average (Supplementary Fig. 2). The effect of aerosol on cloud water is equal throughout the day, with a decrease in cloud water with less aerosol. Even though the cloud water has the highest concentrations below the 0-degree Celsius line, the largest differences between clean and polluted are centered around the 0-degree level (mountain 0-degree line is not shown as it overlaps with the lowland 0-degree line). The impact of aerosol on the snow mixing ratio shows a strong negative field in the morning (more snow in polluted versus clean conditions), while in the afternoon the clean simulations have a higher snow mixing ratio. Rain mostly follows the large snow differences below the freezing line, indicating falling and melting snow that is precipitated out. For graupel in the polluted simulation in the mountains, the mixing ratio is higher than in the clean simulation earlier in the day (until around 15:00) compared to the lowlands.

The graupel and snow differences between the lowlands and mountains indicate stronger and more effective ice formation and growth in the polluted simulations in the mountains compared to the lowlands. Figure 4 shows the change in the vertical temperature profile between clean and polluted conditions for the extreme precipitation events, in addition to the number of activated cloud droplets for the different conditions in the mountains and the lowlands. Results are shown for the lowest 6 km around the 0-degree level. In the mountains, polluted conditions are generally colder, and the elevation of the freezing line is slightly reduced. In addition, a higher number of CCN are activated in the mountains and the number of droplets above the freezing line is increased in polluted conditions, contributing to the

increase in snow formation. Once ice starts to form, riming and the Bergeron–Findeisen process may lead to rapid ice crystal growth and accelerate the precipitation processes.

When cloud water transitions to ice, latent heat is released and buoyancy increases. Figure 5 shows how the vertical updraft is affected by the change in aerosols in the lowlands and in the mountains. The largest differences are situated from 5 to 10 km, well above the freezing level. Similar to the snow mixing ratio response to aerosol, the updrafts are strongly affected by aerosol during the first half of the day, while the clean simulation has higher updrafts in the afternoon (Fig. 5f). The increase in updrafts contributes to more snow production causing an intensification of precipitation. In the lowlands, the change in updrafts between clean and polluted conditions is less than over the mountains (Fig. 5b) indicating a slower ice formation process and thus a lower impact on the precipitation.

The effect of increased updraft is also evident in the RH in the mountains, where the polluted simulation has higher RH up to 10 km elevation contributing to growth of snow. The results also show a depletion of available humidity throughout the day in the polluted simulation, and after the time of peak convective precipitation around 18:00 there is more humidity in the clean simulations. Even though the RH changes throughout the day, the effect of pollution on temperature is almost constant. The polluted simulations in the mountains are colder throughout the day below 10 km, and warmer above. In the lowlands the polluted simulation shows on average more RH throughout the day, and only a small impact on temperature above 2 km.

4. Discussion and Conclusions

The present study demonstrates the highly non-linear and complex responses of extreme precipitation to changes in aerosol concentration. Running a regional climate model with convection permitting resolution, we find contrasting impacts of aerosol on extreme precipitation between the lowlands (below 150 m elevation) and the mountains (above 150 m) in our simulated region in Germany. In the mountains, daily extreme precipitation is reduced in cleaner conditions. This is also supported by observations in a period of rapidly increasing aerosol emissions (until the mid-1980s); both mean precipitation (Napoli et al., 2019) and Rx1day (this study) show stronger increases in the mountains than in the lowlands. Conversely, from the 1990s as the air got cleaner, we find the opposite response: a negative Rx1day trend in the mountains and a continued increase in the lowlands.

Analyzing diurnal and sub-daily timescales we find that on average, these events typically last 8–9 hours in the mountains and 6–7 hours in the lowlands. In the lowlands, cleaner air with less aerosols is associated with more precipitation accumulated over the day, and the precipitation peak is controlled by convective activity is reached earlier than in polluted conditions (shown here and in Alterskjær et al. in review), suggesting a more efficient precipitation process. Meanwhile, in the mountains, it precipitates less compared to polluted conditions during the day, until the afternoon. The peak convective activity in the afternoon is however substantially stronger in cleaner air. This means that although daily accumulated extreme events are less intense under clean conditions, cleaner air produces more intense,

shorter-duration sub-daily extreme events than polluted conditions in the mountains. This pattern is evident across the three highest percentiles examined here (99, 99.7, and 99.9).

Analyzing the effect of increased aerosol for extreme precipitation data above the 99.7 percentile (~ 21 events, corresponding to Rx1day), results at the diurnal and sub-daily timescale reveal that in the mountains we see a consistent tendency that more aerosols lead to more cloud droplets activated, and more cloud droplets above the 0-degree line to freeze. Supplementary Fig. 4 shows that although the mean temperature difference is similar (0.05 degrees) between the mountains and lowlands, the colder temperature in the mountains lies higher in the atmosphere. This leads to more favorable conditions for ice and snow production under polluted conditions in the mountains, in turn leading to more updrafts and even increased snow production depleting access to vapor (compared to clean conditions) in the afternoon.

Orographic effects also impact precipitation on different timescales. While mountains enchase continuous precipitation (longer than 1 hour) causing a positive orographic effect, however for hourly peak convective precipitation mountain suppress the intensity. On hourly time maximum, associated with convective peaks, cleaner air has the same increasing effect over the elevations. Global warming has also been shown to cause a higher increase in extreme precipitation at hourly and 10-minute time scale compared to daily (Hodnebrog et al., 2019). The added effects of increased hourly precipitation from both cleaner air and global warming increase the risk of flash flooding and landslides, leading to potential damage downstream (Archer and Fowler, 2018).

The results presented here show that trends in mean or extreme precipitation under global warming may depend on elevation in regions with changing aerosol loading. Aerosol influences can differ between lowlands and mountains, which may help explain the stronger increases in lowland precipitation trends compared with mountain regions found in Pepin et al. (2022). The effects may also be different in other regions of the world. Separating the lowlands from mountains is therefore necessary to understand the change in precipitation with global warming in areas with aerosol changes. More studies are needed to explore aerosol impacts on extreme precipitation using regional high-resolution models with complex orography (and perhaps stronger contrasts in orography than included in this study) to capture elevation-dependent aerosol-precipitation processes. Current regional climate models, such as those in CORDEX (the Coordinated Regional Downscaling Experiment)(Gutowski Jr. et al., 2016), generally do not include aerosol trends, which limits their ability to reproduce observed temperature and precipitation changes (Schumacher et al., 2024; Steensen et al., 2025; Vautard et al., 2021). The next generation of CORDEX simulations will however include aerosol changes (Katragkou et al., 2024), which is promising. Applying high-resolution, aerosol-aware regional models will be essential for understanding precipitation extremes in complex terrain and improving regional climate projections.

Declarations

Competing Interests

The authors have no relevant financial or non-financial interests to disclose.

Funding

This work has been supported by the EPIC project, grant number 314074.

Author Contributions

All authors contributed to the study conception, analysis and design. Model simulations and figures have been done by Birthe Marie Steensen. The first draft of the manuscript was written by Birthe Marie Steensen and all authors commented on previous versions of the manuscript. All authors read and approved the final manuscript.

Data Availability

The WRF simulations generated and analyzed during the current study are available in the EPIC repository, DOI: 10.11582/2025.6mzrm08

References

1. Albrecht BA (1989) Aerosols, Cloud Microphysics, and Fractional Cloudiness. Science 245:1227–1230. https://doi.org/10.1126/science.245.4923.1227
2. Altaratz O, Koren I, Remer LA, Hirsch E (2014) Review: Cloud invigoration by aerosols—Coupling between microphysics and dynamics. Atmospheric Res 140–141:38–60. https://doi.org/10.1016/j.atmosres.2014.01.009
3. Andrews T, Forster PM, Boucher O, Bellouin N, Jones A (2010) Precipitation, radiative forcing and global temperature change. Geophys Res Lett 37:2010GL043991. https://doi.org/10.1029/2010GL043991
4. Archer DR, Fowler HJ (2018) Characterising flash flood response to intense rainfall and impacts using historical information and gauged data in Britain. J Flood Risk Manag 11. https://doi.org/10.1111/jfr3.12187
5. Ban N, Caillaud C, Coppola E, Pichelli E, Sobolowski S, Adinolfi M, Ahrens B, Alias A, Anders I, Bastin S, Belušić D, Berthou S, Brisson E, Cardoso RM, Chan SC, Christensen OB, Fernández J, Fita L, Frisius T, Gašparac G, Giorgi F, Goergen K, Haugen JE, Hodnebrog Ø, Kartsios S, Katragkou E, Kendon EJ, Keuler K, Lavin-Gullon A, Lenderink G, Leutwyler D, Lorenz T, Maraun D, Mercogliano P, Milovac J, Panitz H-J, Raffa M, Remedio AR, Schär C, Soares PMM, Srnec L, Steensen BM, Stocchi P, Tölle MH, Truhetz H, Vergara-Temprado J, De Vries H, Warrach-Sagi K, Wulfmeyer V, Zander MJ (2021) The

first multi-model ensemble of regional climate simulations at kilometer-scale resolution, part I: evaluation of precipitation. Clim Dyn 57:275–302. https://doi.org/10.1007/s00382-021-05708-w

6. Borga M, Vezzani C, Fontana GD (2005) Regional Rainfall Depth–Duration–Frequency Equations for an Alpine Region. Nat Hazards 36:221–235. https://doi.org/10.1007/s11069-004-4550-y
7. Choudhury G, Tyagi B, Singh J, Sarangi C, Tripathi SN (2019) Aerosol-orography-precipitation – A critical assessment. Atmos Environ 214:116831. https://doi.org/10.1016/j.atmosenv.2019.116831
8. Eirund GK, Van Drossaart S, Brem BT, Dedekind Z, Karrer Y, Stoll M, Lohmann U (2022) Aerosol–cloud–precipitation interactions during a Saharan dust event – A summertime case-study from the Alps. Q J R Meteorol Soc 148:943–961. https://doi.org/10.1002/qj.4240
9. Formetta G, Marra F, Dallan E, Zaramella M, Borga M (2022) Differential orographic impact on sub-hourly, hourly, and daily extreme precipitation. Adv Water Resour 159:104085. https://doi.org/10.1016/j.advwatres.2021.104085
10. Gaume E, Bain V, Bernardara P, Newinger O, Barbuc M, Bateman A, Blaškovičová L, Blöschl G, Borga M, Dumitrescu A, Daliakopoulos I, Garcia J, Irimescu A, Kohnova S, Koutroulis A, Marchi L, Matreata S, Medina V, Preciso E, Sempere-Torres D, Stancalie G, Szolgay J, Tsanis I, Velasco D, Viglione A (2009) A compilation of data on European flash floods. J Hydrol 367:70–78. https://doi.org/10.1016/j.jhydrol.2008.12.028
11. Gutowski WJ Jr., Giorgi F, Timbal B, Frigon A, Jacob D, Kang H-S, Raghavan K, Lee B, Lennard C, Nikulin G, O'Rourke E, Rixen M, Solman S, Stephenson T, Tangang F (2016) WCRP COordinated Regional Downscaling EXperiment (CORDEX): a diagnostic MIP for CMIP6. Geosci. Model Dev 9:4087–4095. https://doi.org/10.5194/gmd-9-4087-2016
12. Hersbach H, Bell B, Berrisford P, Hirahara S, Horányi A, Muñoz-Sabater J, Nicolas J, Peubey C, Radu R, Schepers D, Simmons A, Soci C, Abdalla S, Abellan X, Balsamo G, Bechtold P, Biavati G, Bidlot J, Bonavita M, Chiara G, Dahlgren P, Dee D, Diamantakis M, Dragani R, Flemming J, Forbes R, Fuentes M, Geer A, Haimberger L, Healy S, Hogan RJ, Hólm E, Janisková M, Keeley S, Laloyaux P, Lopez P, Lupu C, Radnoti G, Rosnay P, Rozum I, Vamborg F, Villaume S, Thépaut J (2020) The ERA5 global reanalysis. Q J R Meteorol Soc 146:1999–2049. https://doi.org/10.1002/qj.3803
13. Hodnebrog Ø, Marelle L, Alterskjær K, Wood RR, Ludwig R, Fischer EM, Richardson TB, Forster PM, Sillmann J, Myhre G (2019) Intensification of summer precipitation with shorter time-scales in Europe. Environ Res Lett 14:124050. https://doi.org/10.1088/1748-9326/ab549c
14. Hoesly RM, Smith SJ, Feng L, Klimont Z, Janssens-Maenhout G, Pitkanen T, Seibert JJ, Vu L, Andres RJ, Bolt RM, Bond TC, Dawidowski L, Kholod N, Kurokawa J, Li M, Liu L, Lu Z, Moura MCP, O'Rourke PR, Zhang Q (2018) Historical (1750–2014) anthropogenic emissions of reactive gases and aerosols from the Community Emissions Data System (CEDS). Geosci Model Dev 11:369–408. https://doi.org/10.5194/gmd-11-369-2018
15. Katragkou E, Sobolowski SP, Teichmann C, Solmon F, Pavlidis V, Rechid D, Hoffmann P, Fernandez J, Nikulin G, Jacob D (2024) Delivering an Improved Framework for the New Generation of CMIP6-

Driven EURO-CORDEX Regional Climate Simulations. Bull Am Meteorol Soc 105:E962–E974. https://doi.org/10.1175/BAMS-D-23-0131.1

16. Kendon EJ, Prein AF, Senior CA, Stirling A (2021) Challenges and outlook for convection-permitting climate modelling. Philos Trans R Soc Math Phys Eng Sci 379:20190547. https://doi.org/10.1098/rsta.2019.0547
17. Klein Tank AMG, Wijngaard JB, Können GP, Böhm R, Demarée G, Gocheva A, Mileta M, Pashiardis S, Hejkrlik L, Kern-Hansen C, Heino R, Bessemoulin P, Müller-Westermeier G, Tzanakou M, Szalai S, Pálsdóttir T, Fitzgerald D, Rubin S, Capaldo M, Maugeri M, Leitass A, Bukantis A, Aberfeld R, Van Engelen AFV, Forland E, Mietus M, Coelho F, Mares C, Razuvaev V, Nieplova E, Cegnar T, Antonio López J, Dahlström B, Moberg A, Kirchhofer W, Ceylan A, Pachaliuk O, Alexander LV, Petrovic P (2002) Daily dataset of 20th-century surface air temperature and precipitation series for the European Climate Assessment: EUROPEAN TEMPERATURE AND PRECIPITATION SERIES. Int J Climatol 22:1441–1453. https://doi.org/10.1002/joc.773
18. Kreienkamp F, Sjoukje P, Tradowsky JS, Kew SF, Lorenz P, Arrighi J, Belleflamme A, Bettmann T, Steven C, Chan SC, Ciavarella A, De Cruz L, De Vries H, Demuth N et al (2021) Rapid attribution of heavy rainfall events leading to the severe flooding in Western Europe during July 2021 (World Weather Artribution).
19. Lucas-Picher P, Argüeso D, Brisson E, Tramblay Y, Berg P, Lemonsu A, Kotlarski S, Caillaud C (2021) Convection -permitting modeling with regional climate models: Latest developments and next steps. WIREs Clim Change 12:e731. https://doi.org/10.1002/wcc.731
20. Lund MT, Myhre G, Haslerud AS, Skeie RB, Griesfeller J, Platt SM, Kumar R, Myhre CL, Schulz M (2018) Concentrations and radiative forcing of anthropogenic aerosols from 1750 to 2014 simulated with the Oslo CTM3 and CEDS emission inventory. Geosci Model Dev 11:4909–4931. https://doi.org/10.5194/gmd-11-4909-2018
21. Myhre G, Alterskjær K, Stjern CW, Hodnebrog Ø, Marelle L, Samset BH, Sillmann J, Schaller N, Fischer E, Schulz M, Stohl A (2019) Frequency of extreme precipitation increases extensively with event rareness under global warming. Sci Rep 9:16063. https://doi.org/10.1038/s41598-019-52277-4
22. Napoli A, Crespi A, Ragone F, Maugeri M, Pasquero C (2019) Variability of orographic enhancement of precipitation in the Alpine region. Sci Rep 9:13352. https://doi.org/10.1038/s41598-019-49974-5
23. Pepin NC, Arnone E, Gobiet A, Haslinger K, Kotlarski S, Notarnicola C, Palazzi E, Seibert P, Serafin S, Schöner W, Terzago S, Thornton JM, Vuille M, Adler C (2022) Climate Changes and Their Elevational Patterns in the Mountains of the World. Rev. Geophys. 60, e2020RG000730. https://doi.org/10.1029/2020RG000730
24. Prein A, Rasmussen R, Stephens G (2017) Challenges and Advances in Convection-Permitting Climate Modeling. Bull Am Meteorol Soc 98:1027–1030. https://doi.org/10.1175/BAMS-D-16-0263.1
25. Roe GH (2005) OROGRAPHIC PRECIPITATION. Annu. Rev Earth Planet Sci 33:645–671. https://doi.org/10.1146/annurev.earth.33.092203.122541

26. Rosenfeld D, Dai J, Yu X, Yao Z, Xu X, Yang X, Du C (2007) Inverse Relations Between Amounts of Air Pollution and Orographic Precipitation. Science 315:1396–1398. https://doi.org/10.1126/science.1137949
27. Samset BH (2022) Aerosol absorption has an underappreciated role in historical precipitation change. Commun Earth Environ 3:242. https://doi.org/10.1038/s43247-022-00576-6
28. Schumacher DL, Singh J, Hauser M, Fischer EM, Wild M, Seneviratne SI (2024) Exacerbated summer European warming not captured by climate models neglecting long-term aerosol changes. Commun Earth Environ 5:182. https://doi.org/10.1038/s43247-024-01332-8
29. Skamarock WC, Klemp JB (2008) A time-split nonhydrostatic atmospheric model for weather research and forecasting applications. J Comput Phys 227:3465–3485. https://doi.org/10.1016/j.jcp.2007.01.037
30. Skeie RB, Myhre G, Hodnebrog Ø, Cameron-Smith PJ, Deushi M, Hegglin MI, Horowitz LW, Kramer RJ, Michou M, Mills MJ, Olivié DJL, Connor FMO, Paynter D, Samset BH, Sellar A, Shindell D, Takemura T, Tilmes S, Wu T (2020) Historical total ozone radiative forcing derived from CMIP6 simulations. Npj Clim Atmospheric Sci 3:32. https://doi.org/10.1038/s41612-020-00131-0
31. Squires P (1958) The Microstructure and Colloidal Stability of Warm Clouds. Tellus 10:262–271. https://doi.org/10.1111/j.2153-3490.1958.tb02012.x
32. Steensen BM, Myhre G, Hodnebrog Ø, Alterskjær K (2025) How climate models reproduce the observed increase in extreme precipitation over Europe. PLOS Clim 4:e0000442. https://doi.org/10.1371/journal.pclm.0000442
33. Thompson G, Eidhammer T (2014) A Study of Aerosol Impacts on Clouds and Precipitation Development in a Large Winter Cyclone. J Atmospheric Sci 71:3636–3658. https://doi.org/10.1175/JAS-D-13-0305.1
34. Thompson G, Field PR, Rasmussen RM, Hall WD (2008) Explicit Forecasts of Winter Precipitation Using an Improved Bulk Microphysics Scheme. Part II: Implementation of a New Snow Parameterization. Mon Weather Rev 136:5095–5115. https://doi.org/10.1175/2008MWR2387.1
35. Thompson G, Tewari M, Ikeda K, Tessendorf S, Weeks C, Otkin J, Kong F (2016) Explicitly-coupled cloud physics and radiation parameterizations and subsequent evaluation in WRF high-resolution convective forecasts. Atmospheric Res 168:92–104. https://doi.org/10.1016/j.atmosres.2015.09.005
36. Twomey S (1977) The Influence of Pollution on the Shortwave Albedo of Clouds. J Atmospheric Sci 34:1149–1152. https://doi.org/10.1175/1520-0469(1977)034%3C1149:TIOPOT%3E2.0.CO;2
37. Vautard R, Kadygrov N, Iles C, Boberg F, Buonomo E, Bülow K, Coppola E, Corre L, Van Meijgaard E, Nogherotto R, Sandstad M, Schwingshackl C, Somot S, Aalbers E, Christensen OB, Ciarlo JM, Demory M, Giorgi F, Jacob D, Jones RG, Keuler K, Kjellström E, Lenderink G, Levavasseur G, Nikulin G, Sillmann J, Solidoro C, Sørland SL, Steger C, Teichmann C, Warrach-Sagi K, Wulfmeyer V (2021) Evaluation of the Large EURO-CORDEX Regional Climate Model Ensemble. J. Geophys. Res. Atmospheres 126, e2019JD032344. https://doi.org/10.1029/2019JD032344

38. Wild M (2009) Global dimming and brightening: A review. J Geophys Res Atmos. https://doi.org/10.1029/2008JD011470. 114, 2008JD011470
39. Zou A, Yang Y, Wang H, Wang P, Liao H (2025) Aerosol Decline Accelerates the Increasing Extreme Precipitation in China. Geophys Res Lett 52. https://doi.org/10.1029/2024GL113887. e2024GL113887
40. Zubler EM, Lohmann U, Lüthi D, Schär C, Muhlbauer A (2011) Statistical Analysis of Aerosol Effects on Simulated Mixed-Phase Clouds and Precipitation in the Alps. J Atmospheric Sci 68:1474–1492. https://doi.org/10.1175/2011JAS3632.1

Figures

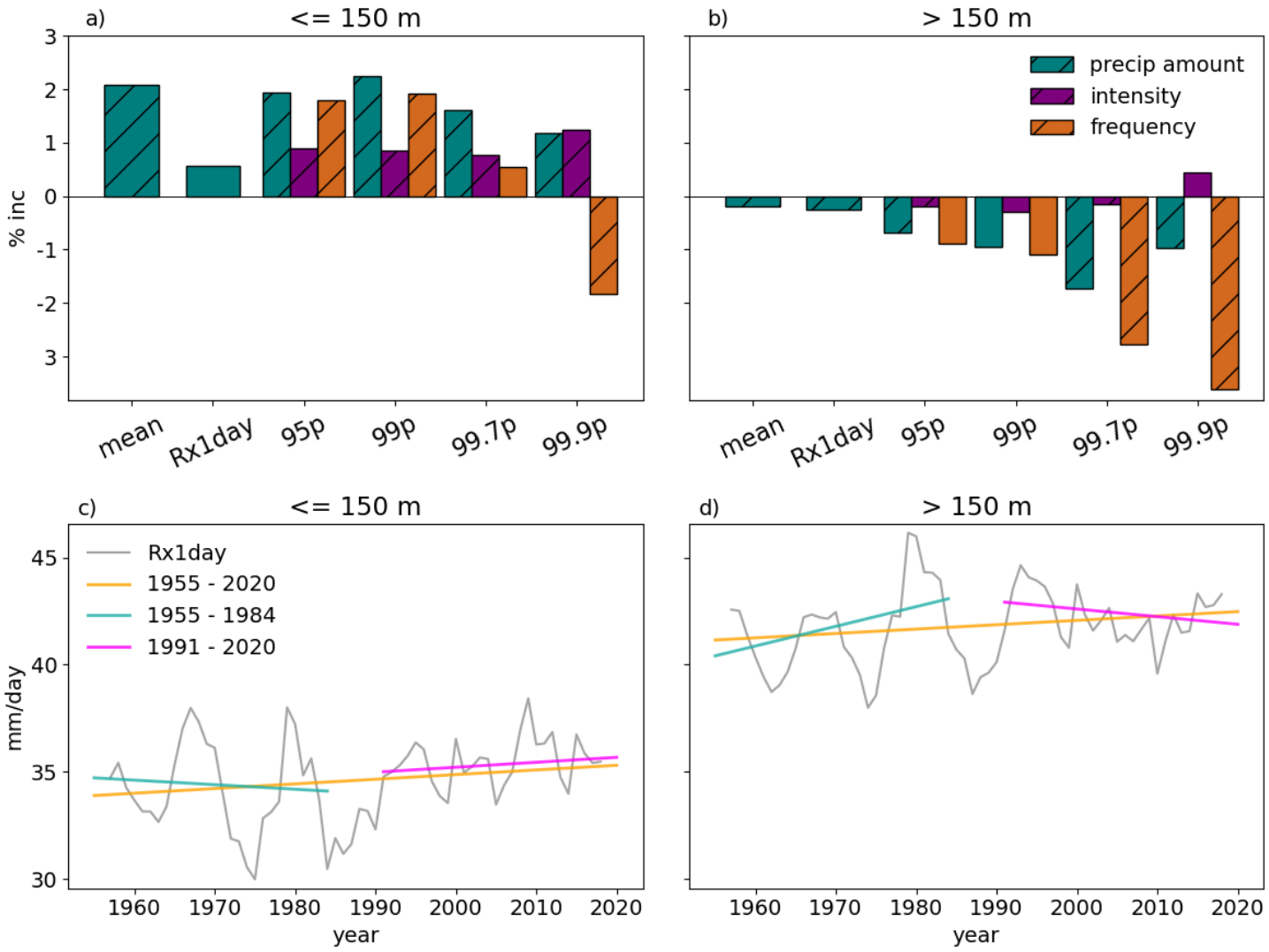


Figure 1

Top row shows modelled relative change in precipitation amount (green), intensity (purple) and frequency (orange) of mean and extreme precipitation between the polluted and clean simulations from the convective permitting WRF simulations for grid cells below (a) and above 150 m elevation (b).

Hatched bars show statistical significance (p<0.05) using the two-sided Wilcoxon test. Bottom row shows observed five-year running mean Rx1day (grey) from 1955-2020, as well as linear trends over the full period (orange), from 1955-1984 (light green) and from 1991-2020 (pink), for stations below (c) and above 150 m elevation (d), respectively.

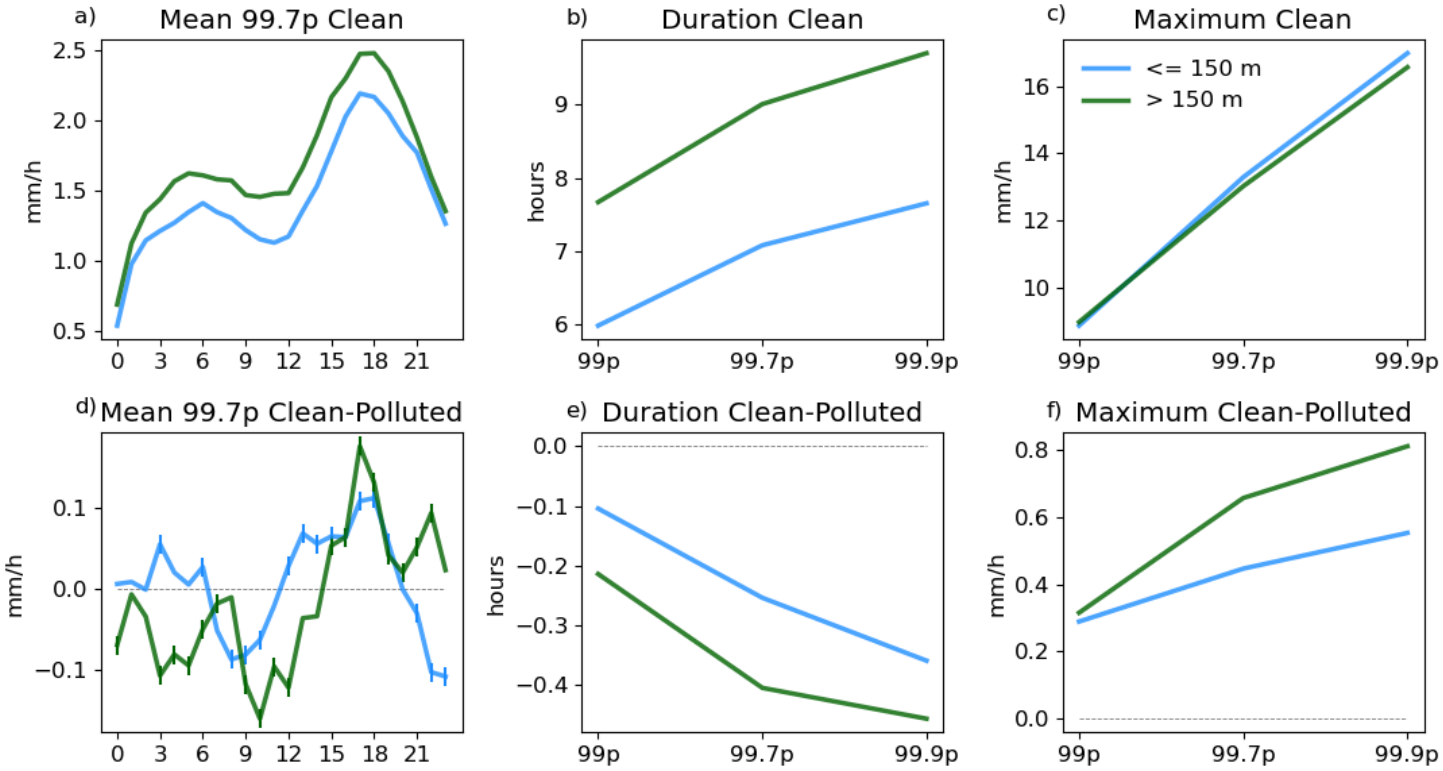


Figure 2

Above, the diurnal hourly precipitation a) averaged for the days over the 99.7 percentile threshold in the clean simulation, b) the duration of precipitation (hours >= 1 mm/h) for the 99, 99.7 and 99.9 percentile and c) the maximum hourly precipitation during the days above the thresholds for the same three percentiles, for grid cells below 150 m (blue) and above 150 m (green). Below, the difference between clean and polluted for the same statistics as above, where positive values indicate an increase with cleaner air. Vertical line markers in d) show where the difference between clean and polluted simulations is statistically significant (p<0.05) with the two-sided Wilcoxon test

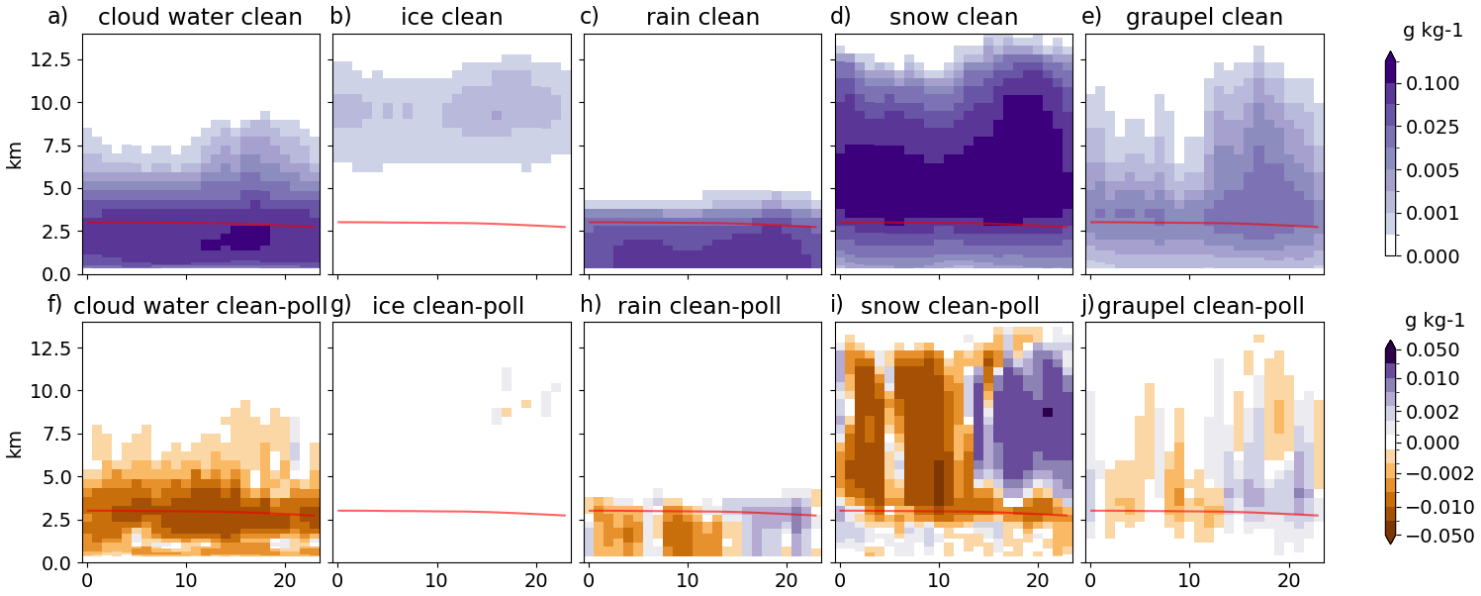


Figure 3

Top: The average diurnal mixing ratio (g kg-1) in clean conditions over the grid cells above 150 m elevation for the hydrometeors included in the Thompson scheme averaged for days over the 99.7 percentile threshold. Bottom: The change in mixing ratio of the same hydrometeors between clean and polluted conditions. Notice the logarithmic increments in the color bars. The red line represents the temperature level of 0-degrees C in the clean simulations

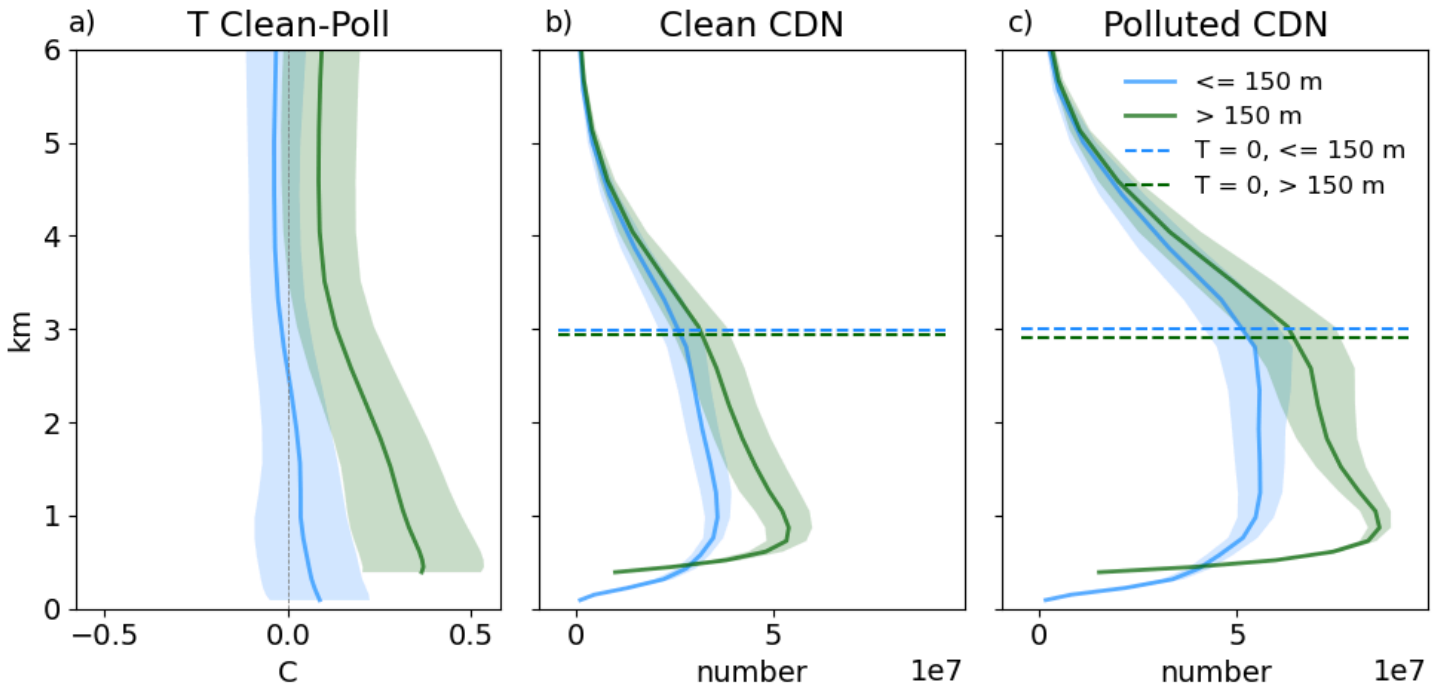


Figure 4

For the lowest 6 km daily averag for the days over the 99.7 percentile, a) temperature profile difference between clean and polluted simulations. b) and c) the number of activated cloud drops (CDN) for the clean and polluted simulations respectively in the lowlands (<= 150 m) in blue, and mountains (> 150 m) in green. Shading represents the mean standard deviation between the events over the grid cells. Dashed lines in b) and c) show the elevation of the daily mean 0-degree Celsius line for the different simulations, linearly interpolated from model levels to the closest 0.25 degree providing a resolution of <5 m accuracy

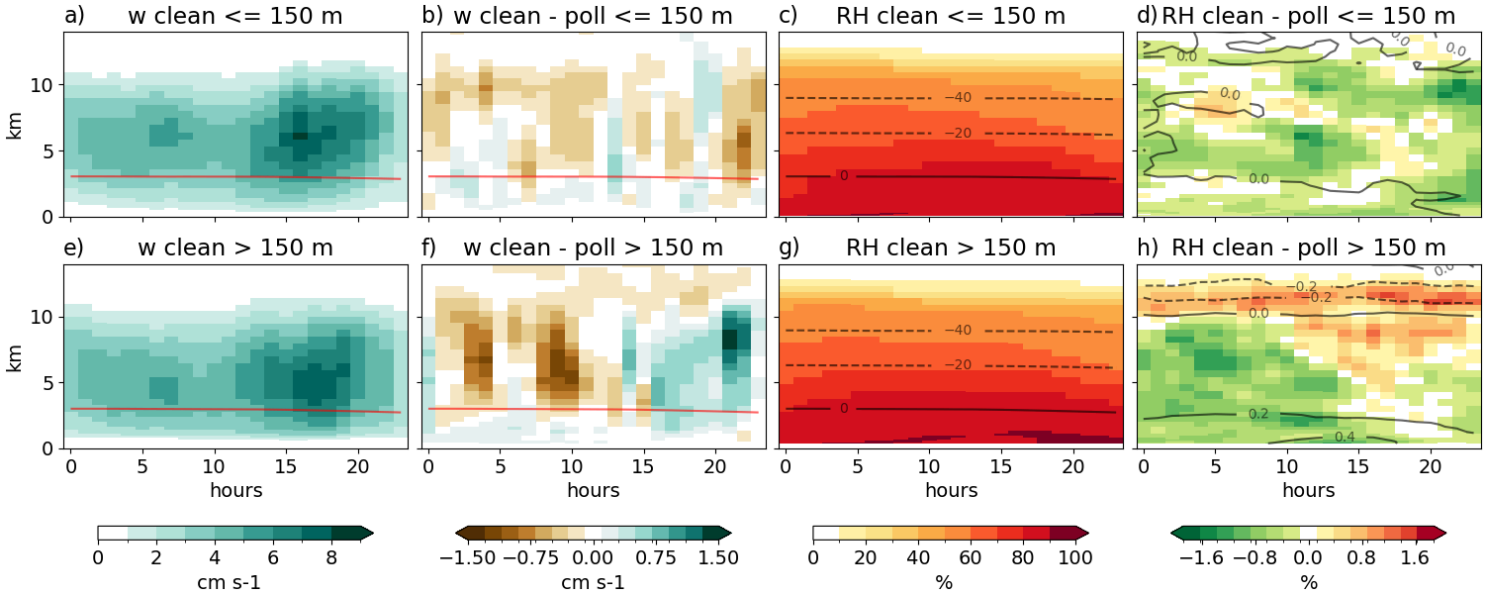


Figure 5

Diurnal variation in updraft and relative humidity for the days with precipitation above the 99.7 percentile. Lowlands above and mountain grid cells below. The updraft is shown for clean conditions (a, e) and its change between clean and polluted conditions (b, f). The line of 0-degree Celsius is shown in red for clean conditions. RH with temperature in black contours in Celsius (with negative values in dashed) in clean conditions for lowlands (c) and in the mountains (g), the difference in RH and temperature in black contours (with negative values in dashed) between clean and polluted conditions for lowlands (d) and mountains (h)

Supplementary Files

This is a list of supplementary files associated with this preprint. Click to download.

- supplementaryelevation.docx